Thiadizoloquinoxaline-Based Low-Bandgap Conjugated Polymers as Ambipolar Semiconductors for Organic Field Effect Transistors

ARTICLE *in* CHEMISTRY OF MATERIALS · SEPTEMBER 2014

Impact Factor: 8.35 · DOI: 10.1021/cm502563t

7 AUTHORS, INCLUDING:

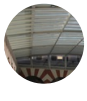

Cunbin An
Max Planck Institute for Polymer Research
14 PUBLICATIONS **79** CITATIONS
SEE PROFILE

Dan Li
Max Planck Institute for Polymer Research
7 PUBLICATIONS **87** CITATIONS
SEE PROFILE

Tomasz Marszalek
Max Planck Institute for Polymer Research
29 PUBLICATIONS **182** CITATIONS
SEE PROFILE

Martin Baumgarten
Max Planck Institute for Polymer Research
279 PUBLICATIONS **4,309** CITATIONS
SEE PROFILE

CHEMISTRY OF MATERIALS

Article

pubs.acs.org/cm

Thiadizoloquinoxaline-Based Low-Bandgap Conjugated Polymers as Ambipolar Semiconductors for Organic Field Effect Transistors

Cunbin An, Mengmeng Li, Tomasz Marszalek, Dan Li, Rüdiger Berger, Wojciech Pisula, and Martin Baumgarten*

Max Planck Institute for Polymer Research, Ackermannweg 10, 55128 Mainz, Germany

Supporting Information

ABSTRACT: Two novel conjugated polymers with high molecular weight, **PBDTTQ-3** and **PAPhTQ**, were synthesized by tuning alkyl chains and alternating the electron-donating ability of the thiadiazoloquinoxaline (TQ) moiety. Both polymers have excellent solubility in common organic solvents. UV−vis−NIR absorption and cyclic voltammetry indicate a bandgap of (0.76 eV) and high electron affinity level (−4.08 eV) for **PBDTTQ-3**. Two dimensional wide-angle X-ray scattering shows that both polymers are only poorly ordered in the bulk but possess a close π-stacking distance of 0.36 nm. Despite the disorder in thin film observed by grazing incidence wide-angle X-ray scattering, **PBDTTQ-3** exhibits good ambipolar transport, with a maximum hole mobility of 0.22 $cm^2\ V^{-1}\ s^{-1}$ and comparable electron mobility of 0.21 $cm^2\ V^{-1}\ s^{-1}$.

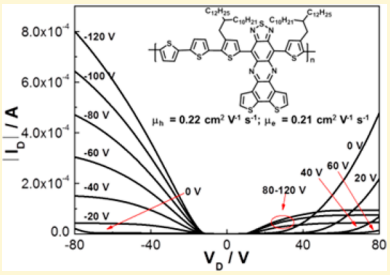

INTRODUCTION

Ambipolar organic field-effect transistors (OFETs) that transport simultaneously holes and electrons have attracted attention in recent years, owing to their application in complementary metal−oxide semiconductors (CMOS) logic circuits and organic light-emitting transistors.[1−4] Strong acceptors were widely used to create high performance alternating donor (D)−acceptor (A) ambipolar semiconductors because of their electron-deficient nature. Due to the trapping of electrons at the semiconductor/dielectric interface and the scarcity of high-electron-affinity building blocks,[5] only few acceptors have been used to design ambipolar polymers with hole and electron mobilities both above 0.1 $cm^2\ V^{-1}\ s^{-1}$ such as benzobisthiadiazole (BBT),[6−8] naphthalene diimide (NDI),[9] diketopyrrolopyrrole(DPP),[10−12] isoindigo (IID),[13] and benzodifurandione-based oligo(*p*-phenylenevinylene) (BDOPV).[14]

Thiadiazoloquinoxalines (TQs) are also strong planar acceptors. The design, synthesis, and characterization of TQ-containing polymers have undergone important progress in the past decade.[15−31] Most TQ-based polymers have been reported to show hole transport, while only few of them were presented as ambipolar semiconductors.[27,32,33] However, these systems usually exhibited very low mobilities ($\lesssim 10^{-2}\ cm^2\ V^{-1}\ s^{-1}$) in OFETs. Two reasons may lead to low charge carrier mobility and limit their application in optoelectronic devices. The first is the low molecular weight of TQ-containing polymers. It has been proven for conjugated polymers that the degree of microstructural order improves with increasing molecular weight.[34] The second reason is related to the twisting between each building block in the TQ-containing polymer backbone. A typical strategy to increase the solubility and improve the molecular weight of TQ-containing polymers is the attachment of a sufficiently high number of alkyl chains at the repeat unit. However, as a drawback this strategy causes larger torsion angles within the backbone due to steric hindrance of the substituents leading to poor packing and low charge carrier transport of the semiconductor. Therefore, it is important to balance the two aspects to achieve high performance TQ-containing polymers in OFET applications.

Previously, we developed a new highly conjugated TQ core (**BDTTQ**) and successfully constructed two polymers **PBDTTQ-1** and **PBDTTQ-2** (Figure 1) by varying its linkage pattern within the conjugated backbone. The different electron density distributions on the conjugated backbone and deep LUMO levels of both polymers led to their significant difference in device performance. **PBDTTQ-1** did not show any field-effect response, while **PBDTTQ-2** exhibited an ambipolar transport with medium charge carrier mobilities.[33]

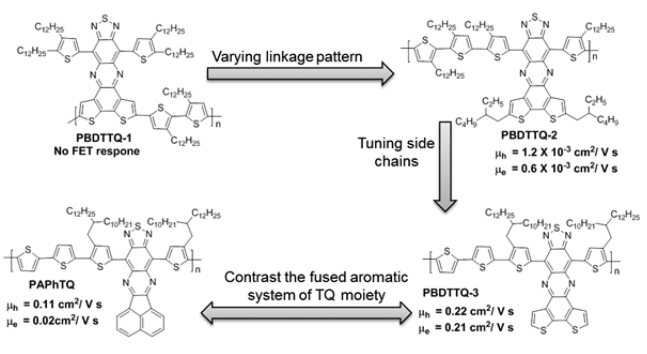

Figure 1. Rational design changes for improving the device performance of TQ-containing polymers.

Received: July 14, 2014
Revised: September 26, 2014
Published: September 26, 2014

Scheme 1. Synthetic Routes to Polymers PBDTTQ-3 and PAPhTQ[a]

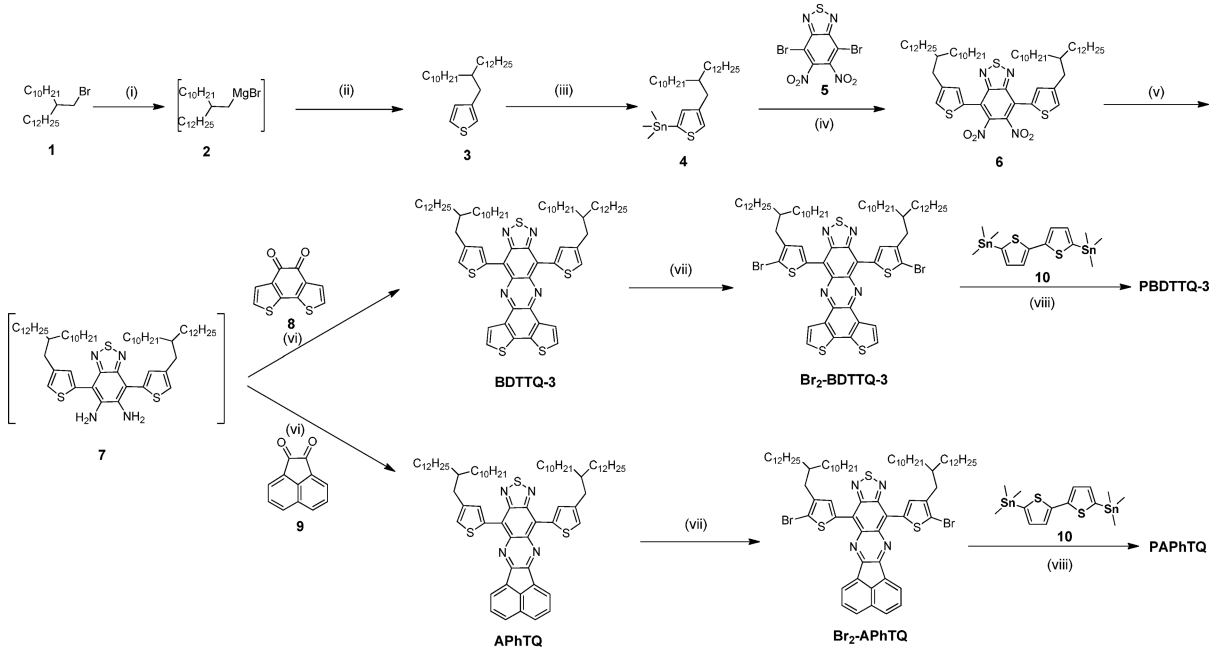

[a]Reagents and conditions: (i) Mg, I_2, THF; (ii) 3-bromothiophene, Ni(dppp)Cl_2, THF, 51%; (iii) TMEDA, *n*-BuLi, THF, $(CH_3)_3SnCl$, 95%; (iv) Pd(PPh_3)Cl_2, THF, 71%; (v) Fe, CH_3COOH; (vi) CH_3COOH, benzo[2,1-*b*:3,4-*b*′]dithiophene-4,5-dione, 71% (two steps); CH_3COOH, acenaphthylene-1,2-dione 62% (two steps); (vii) NBS, THF, 91% for **Br_2-BDTTQ-3**, 91% for **Br_2-APhTQ**; (viii) chlorobenzene, $Pd_2(dba)_3$, tri(*o*-tolyl)phosphine, 76% for **PBDTTQ-3**, 72% for **PAPhTQ**.

But the disordered morphology and low molecular weight of **PBDTTQ-2** was believed to limit its charge transport. Usually, the alkylation or alkoxylation of a TQ segment extends the size of the TQ core. This extension decreases the polymer interactions and limits their packing. Long branched alkyl chains with one methylene group past the branching point have been elaborated in other large π-conjugated acceptors and proven to play a key role not only in increasing the molecular weight and the solubility of the polymers but also in influencing the microstructural morphology and charge carrier transport.[7−9,35,36] To improve the interaction of TQ polymers, we developed a new benzodithiophene condensed TQ unit (**BDTTQ-3**) with excellent solubility in common organic solvents, by removing all of alkyl chains from TQ unit and replacing linear alkyl chains using a pair of 2-decyl-tetradecyl alkyl chains in the neighboring thiophene units. Additionally, another new acenaphthylene condensed TQ core (**APhTQ**) was also developed for comparison with **BDTTQ-3** (Scheme 1).

Herein, we report the design and synthesis of two D−A polymers **PBDTTQ-3** and **PAPhTQ** (Figure 1) and their enhanced device performance compared to **PBDTTQ-2**. For both polymers, 2-decyl-tetradecyl alkyl chains with branching positions one carbon away from the polymer main chain on thiophenes adjacent to the acceptors are crucial for tuning the attractive forces and improving the solubility of the macromolecules. More importantly, this approach minimizes steric interactions and promotes the polymer backbone coplanarity, which facilitates charge carrier transport. In this study, **PBDTTQ-3** shows significantly improved and balanced holes and electron mobilities as high as 0.22 and 0.21 $cm^2\ V^{-1}\ s^{-1}$, respectively. **PAPhTQ** exhibits also ambipolarity with slightly lower maximum mobilities of 0.11 $cm^2\ V^{-1}\ s^{-1}$ for holes and 0.02 $cm^2\ V^{-1}\ s^{-1}$ for electrons. Additionally, the influence of the fused aromatic system in the TQ moiety on the device performance was studied.

EXPERIMENTAL SECTION

Synthetic Details. All chemicals and reagents were used as received from commercial sources without further purification unless stated otherwise. Intermediates 2-decyl-tetradecyl bromide (**1**),[37] 4,7-dibromo-5,6-dinitro-2,1,3-benzothiadiazole (**5**),[33] benzo[2,1-*b*:3,4-*b*′]-dithiophene-4,5-dione (**8**),[38] and 5,5′-bis(trimethylstannyl)-2,2′-bithiophene (**12**)[39]were prepared according to the literature procedures.

3-(2-Decyltetradecyl)thiophene (3). Magnesium turnings (0.7 g, 29 mmol), a catalytic amount of iodine, and 30 mL of dry THF were mixed in a 100 mL flask and heated to 80 °C under argon. A solution of 2-decyl-tetradecyl bromide (10 g, 24 mL) in 20 mL of dry THF was added dropwise into the flask within 30 min. The resulting mixture was refluxed overnight and then cooled down to room temperature. The gray solution was transferred into a dry constant pressure funnel and added dropwise into a dry THF (20 mL) solution of 3-bromothiophene (3.9 g, 24 mmol) and Ni(dppp)Cl_2 (316 mg, 0.58 mmol) at room temperature. The mixture was heated to reflux overnight under argon. The mixture was then cooled down and then 1 N HCl was added to quench excess Grignard reagent. The crude product was extracted with diethyl ether (3 × 20 mL). The combined organic phases were dried with $MgSO_4$, and the solvent was removed under reduced pressure to afford dark oil, which was purified by column chromatography eluting with hexane to give 5.1 g (colorless oil, 51%) of compound **3**. ^{1}H NMR: (250 MHz, CD_2Cl_2, ppm) δ 7.25−7.22 (m, 1H), 6.93−6.90 (m, 2H), 2.58−2.55 (d, 2H, J = 7.5 Hz), 1.63−1.58 (m, 1H), 1.35−1.22 (br, 40H), 0.91−0.86 (t, 6H, J = 5.0 Hz, J = 7.5 Hz). ^{13}C NMR (62.5 MHz, CD_2Cl_2, ppm) δ 142.48, 129.24, 125.10, 121.02, 39.38, 35.04, 33.72, 32.38, 30.44, 30.17, 30.14, 30.11, 29.81, 28.99, 23.14, 14.34. HRMS (ESI+): m/z calcd 421.3868, found 421.3874.

2-Trimethylstannyl-4-(2-decyltetradecyl)thiophene (4). 3-(2-Decyltetradecyl)thiophene (3.63 g, 8.63 mmol) and *N*,*N*,*N*′,*N*′-tetramethylethylenediamine (TMEDA, 1.42 mL, 9.49 mmol) were dissolved in 36 mL of anhydrous THF. The mixture was cooled down

dx.doi.org/10.1021/cm502563t | *Chem. Mater.* 2014, 26, 5923−5929

to 0 °C, and *n*-BuLi (5.93 mL, 9.49 mmol, 1.6 M in hexane) was added slowly over 10 min. The resulting solution was stirred for 5 min at 0 °C and warmed to room temperature over 30 min. The mixture was cooled down to 0 °C again, and trimethyltin chloride (9.49 mL, 9.49 mmol, 1 M in hexane) was added dropwise. The mixture was stirred for 30 min at 0 °C and warmed to room temperature. After 2 h, the resulting solution was poured into water and extracted with diethyl ether. The combined organic phases were washed with brine, dried with $MgSO_4$, and filtered. The filtrate was concentrated under reduced pressure to obtain compound **3** (4.8 g, yellow oil, 95%). This crude product was used for the next step without further purification. ^{1}H NMR: (250 MHz, CD_2Cl_2, ppm) δ 7.16 (s, 1H), 6.98 (s, 1H), 2.59−2.56 (d, 2H, J = 7.5 Hz), 1.63−1.58 (m, 1H), 1.34−1.22 (br, 40H), 0.91−0.85 (t, 6H, J = 7.5 Hz), 0.34(s, 9H). ^{13}C NMR (62.5 MHz, CD_2Cl_2, ppm) δ 143.71, 137.73, 137.27, 126.92, 39.56, 34.77, 33.90, 32.51, 30.59, 30.28, 30.25, 29.95, 27.13, 23.27, 14.48, 8.12.

4,7-Bis(4-(2-decyltetradecyl)thiophen-2-yl)-5,6-dinitrobenzo[*c*][1,2,5]thiadiazole (6). 4,7-Dibromo-5,6-dinitrobenzodiazole (**5**) (1.23g, 3.2 mmol), compound **4** (4.30 g, 7.40 mmol), and $Pd(PPh_3)Cl_2$ (225 mg, 0.32 mmol) were dissolved in 40 mL of anhydrous THF under argon. The resulting solution was stirred for 16 h at 80 °C. The solvent was removed under reduced pressure to afford a dark-red oil, which was purified by column chromatography to give 2.42 g (red solid, 71%) of compound **6**. ^{1}H NMR (250 MHz, CD_2Cl_2, ppm) δ 7.34 (s, 2H), 7.32 (s, 2H), 2.65 (d, J = 7.50 Hz, 4H), 1.69−1.63 (m, 2H), 1.29−1.27 (m, 80H), 0.91−0.86 (t, J = 7.50 Hz, J = 5.0 Hz, 12H). ^{13}C NMR (62.5 MHz, CD_2Cl_2, ppm) δ 152.59, 143.57, 141.97, 133.16, 129.45, 127.69, 121.85, 39.40, 34.94, 33.66, 32.37, 30.41, 30.14, 30.10, 29.80, 27.04, 23.13, 14.33. HRMS (ESI+ Na): m/z calcd 1085.6961, found 1085.6981.

BDTTQ-3. Compound **6** (0.5 g, 0.47 mmol) and fine iron powder (311 mg, 5.55 mmol) in acetic acid (15 mL) was stirred for 5 h at 75 °C under argon. The reaction mixture was cooled down to room temperature, precipitated in 5% aqueous NaOH, and extracted with diethyl ether. The combined organic layers were washed with brine and dried with $MgSO_4$, and the solvent was removed under reduced pressure to give corresponding diamine **7** with deep dark oil. This crude product was added into the acetic acid (15 mL) solution of benzo[2,1-*b*:3,4-*b*′]dithiophene-4,5-dione (103 mg, 0.47 mmol). The mixture was heated to 80 °C overnight under argon. After cooling down to room temperature, the mixture was poured into 100 mL of 5% aqueous NaOH and extracted with dichloromethane. The combined organic phases were dried with $MgSO_4$ and filtered. The filtrate was concentrated and purified by column chromatography eluting with hexane dichloromethane (3:1) to give 0.4 g (green solid, two steps 71%) of **BDTTQ-3**. ^{1}H NMR (250 MHz, CD_2Cl_2, ppm) δ 8.86 (d, J = 1.25 Hz, 2H), 8.22 (d, J = 5.0 Hz, 2H), 7.40 (d, J = 5.0 Hz, 2H), 7.13 (d, J = 2.5 Hz, 2H), 2.65 (d, J = 7.50 Hz, 4H),1.82−1.75 (m, 2H), 1.41−1.23 (m, 80H), 0.88−0.82 (t, J = 7.50 Hz, 12H). ^{13}C NMR (62.5 MHz, $CDCl_3$, ppm) δ 151.00, 141.44, 139.73, 137.38, 136.09, 135.58, 135.15, 134.76, 128.13, 127.15, 124.56, 120.42, 39.21, 35.18, 33.60, 32.09, 30.38, 29.96, 29.92, 29.90, 29.87, 29.84, 29.56, 29.53, 26.94, 22.85, 14.28. HRMS (ESI+): m/z calcd 1187.7099, found 1187.7086.

Br_2-BDTTQ-3. **BDTTQ-3** (150 mg, 0.126 mmol) was dissolved in 15 mL of THF at room temperature. NBS (51.7 mg, 0.29 mmol) was carefully added into the solution in small batches under dark. The mixture was stirred for 5 h. After removing the solvent under reduced pressure, the residue was purified by column chromatography to give **Br_2-BDTTQ-3** as a green solid (154 mg, 91%). ^{1}H NMR (250 MHz, $CDCl_3$, ppm) δ 8.56 (s, 2H), 7.62 (d, J = 5.0 Hz, 2H), 7.10 (d, J = 5.0 Hz, 2H), 2.50 (d, J = 7.50 Hz, 4H),1.82−1.74 (m, 2H), 1.25−1.23 (br, 80H), 0.88−0.83 (t, J = 7.50 Hz, 12H). ^{13}C NMR (62.5 MHz, $CDCl_3$, ppm) δ 149.98, 140.17, 138.66, 137.20, 135.56, 134.60, 133.78, 133.71, 126.66, 124.29, 119.34, 118.72, 38.78, 34.30, 33.59, 32.13, 32.11, 30.49, 30.08, 30.03, 29.98, 29.94, 29.88, 29.60, 29.57, 26.86, 22.87, 14.30. HRMS (ESI+): m/z calcd 1343.5310, found 1343.5322.

APhTQ. Compound **6** (0.5 g, 0.47 mmol) and fine iron powder (311 mg, 5.55 mmol) in acetic acid (15 mL) was stirred for 5 h at 75 °C under argon. The reaction mixture was cooled down to room temperature, precipitated in 5% aqueous NaOH, and extracted with diethyl ether. The combined organic layers were washed with brine and dried with $MgSO_4$, and the solvent was removed under reduced pressure to give corresponding diamine **7** with deep dark oil. This crude product was directly added into acetic acid (15 mL) solution of acenaphthylene-1,2-dione (85.6 mg, 0.47 mmol). The mixture was heated to 80 °C overnight under argon. After cooling down to room temperature, the mixture was poured into 100 mL of 5% aqueous NaOH and extracted with dichloromethane. The combined organic phases were dried with $MgSO_4$ and filtered. The filtrate was concentrated and purified by column chromatography eluting with hexane dichloromethane (3:1) to give 0.34 g (green solid, two steps 62%) of **APhTQ**. ^{1}H NMR (250 MHz, CD2Cl2, ppm) δ 8.86 (s, 2H), 8.32 (d, J = 5.0 Hz, 2H), 8.09 (d, J = 7.5 Hz, 2H), 7.81 (t, J = 7.5 Hz, 2H), 7.23 (s, 2H), 2.71 (d, J = 7.50 Hz, 4H), 1.82−1.77 (m, 2H), 1.26−1.23 (br, 80H), 0.87−0.82 (t, J = 7.50 Hz, 12H). ^{13}C NMR (62.5 MHz, $CDCl_3$, ppm) δ 153.19, 151.91, 141.41, 139.34, 135.78, 135.54, 135.50, 131.56, 130.27, 129.64, 128.84, 127.82, 122.64, 122.27, 39.19, 35.16, 33.57, 32.08, 30.33, 29.96, 29.92, 29.89, 29.85, 29.83, 29.54, 29.52, 26.91, 22.84, 14.28. HRMS (ESI+): m/z calcd 1149.7814 found 1149.7826.

Br_2-APhTQ. **APhTQ** (207 mg, 0.18 mmol) was dissolved in 15 mL of THF at room temperature. NBS (73.7 mg, 0.41 mmol) was carefully added into the solution in small batches under dark. The mixture was stirred for 5 h. After removing the solvent under reduced pressure, the residue was purified by column chromatography to give **Br_2-APhTQ** as a green solid (200 mg, 91%). ^{1}H NMR (250 MHz, CD2Cl2, ppm) δ 8.43 (s, 2H), 7.71 (d, J = 10.0 Hz, 2H), 7.42 (d, J = 5.0 Hz, 2H), 7.32 (t, J = 7.5 Hz, 2H), 2.36 (d, J = 5.0 Hz, 4H), 1.75−1.67 (m, 2H), 1.35−1.24 (br, 80H), 0.89−0.80 (t, J = 7.50 Hz, 12H). ^{13}C NMR (62.5 MHz, $CDCl_3$, ppm) δ 152.34, 150.98, 140.17, 138.95, 135.65, 134.67, 134.26, 130.75, 129.98, 129.53, 128.71, 122.73, 120.72, 119.20, 38.73, 34.28, 33.60, 32.11, 32.09, 30.40, 30.01, 29.98, 29.94, 29.91, 29.89, 29.85, 29.57, 29.54, 26.83, 22.85, 14.28. HRMS (ESI+): m/z calcd 1305.6025, found 1305.6067.

PBDTTQ-3. **Br_2-BDTTQ-3** (0.1 mmol), compound **10** (0.1 mmol), and chlorobenzene (8 mL) were placed in a 50 mL Schlenk tube. The mixture was purged with argon for 5 min, and then 5.5 mg of tris(dibenzylideneacetone)dipalladium(0) ($Pd_2(dba)_3$) and 7.3 mg of tri(*o*-tolyl)phosphine ($P(o\text{-tolyl})_3$) were added. Then the mixture was heated up to 110 °C under argon for 3 days. The polymer was end-capped with tributylphenylstannane and bromobenzene in sequence. After cooling to room temperature, the reaction mixture was poured into methanol. The polymer was filtered and subjected to Soxhlet extraction with methanol, acetone, hexane, dichloromethane, and chloroform. The chloroform fraction was collected, and 30 mL of sodium diethyldithiocarbamate aqueous solution (1 g/100 mL) was added; the mixture was heated to 60 °C with vigorous stirring for 2 h. The mixture was separated, and the organic phase was washed with water three times. The chloroform solution was concentrated and precipitated in methanol. The target polymer was collected by filtration and dried in vacuum to afford a black solid 102.7 mg (76%). Molecular weight by GPC: M_n = 76.3K (g/mol), PDI = 3.64. Anal. Calcd for $C_{80}H_{108}N_4S_7$: C, 71.20; H, 8.07; N, 4.15; S, 16.58. Found: C, 70.66; H, 8.38; N, 3.98; S, 16.04.

PAPhTQ. This polymer was prepared from **Br_2-APhTQ** and compound **10** in a procedure similar to that of **PBDTTQ-3** as a black solid, 94.6 mg (72%). Molecular weight by GPC: M_n = 100.9K (g/mol), PDI = 6.48. Anal. Calcd for $C_{82}H_{110}N_4S_5$: C, 75.09; H, 8.45; N, 4.27; S, 12.19. Found: C, 74.73; H, 8.91; N, 4.01; S, 11.61.

RESULTS AND DISCUSSION

Synthesis and Characterization. The synthesis of the two monomers and their corresponding polymers is illustrated in Scheme 1. Grignard reagent **2** was prepared from 2-decyltetradecyl bromide (**1**) and was converted to **4** by first introducing branched alkyl chains via a Kumada coupling then performing stanylation. After Stille coupling reaction between **4** and **5**, the corresponding dinitro **6** was obtained. Diamine **7**

Table 1. Molecular Weights, Optical Absorption, Electrochemical Properties, and Field-Effect Mobilities of PBDTTQ-3 and PAPhTQ

polymer	M_n/M_w (kg/mol)[a]	T_d (°C)[b]	λ_{abs} (nm) soln.[c]	λ_{abs} (nm) film[d]	E_g^{opt} (eV)[d]	IP (eV)[e]	EA (eV)[e]	$\mu_{h,max,ave}$ ($cm^2 V^{-1} s^{-1}$)	$\mu_{e,max,ave}$ ($cm^2 V^{-1} s^{-1}$)
PBDTTQ-3	76.3/277.3	415	1206	1270	0.76	−5.05	−4.08	0.22, 0.19 (±0.03)	0.21, 0.10 (±0.07)
PAPhTQ	100.9/654.5	415	1005	1072	0.99	−5.10	−3.94	0.11, 0.10 (±0.02)	0.02, 0.02 (±0.01)

[a]Determined by GPC in THF using polystyrene standards. [b]Temperature of decomposition corresponding to 5% weight loss from TGA analysis under N_2 with the heating rate of 10 °C/min. [c]Dissolved in choloform ($c = 10^{-5}$ M). [d]Drop-cast from choloform solution (2 mg/mL). [e]IP and EA were estimated from the onsets of the first oxidation and reduction peak, while the potentials were determined using ferrocene (Fc) as standard by empirical formulas IP/EA = $-(E_{ox/red}^{onset} - E_{Fc/Fc+}^{1/2} + 4.8)$ eV wherein $E_{Fc/Fc+}^{1/2} = 0.40$ eV.

was synthesized by reduction of compound **6** and then directly converted to the corresponding monomers **BDTTQ-3** and **APhTQ** via a condensation coupling with benzo[2,1-*b*:3,4-*b*′]dithiophene-4,5-dione (**8**) and acenaphthylene-1,2-dione (**9**). Consequently, monomers **Br_2-BDTTQ-3** and **Br_2-APhTQ** were then obtained by dibromination of **BDTTQ-3** and **APhTQ**. Both polymers were prepared via Stille coupling between **Br_2-BDTTQ-3** or **Br_2-APhTQ** and distannylbithiophene **12**. The detailed synthesis is depicted in the Experimental Section.

Both polymers possess good solubility in chloroform, tetrahydrofuran, and chlorobenzene. The number-average molecular weights (M_n) of the polymers were 76.3 and 100.9 K, with a polydispersity index (PDI) of 3.64 and 6.48 for **PBDTTQ-3** and **PAPhTQ**, respectively, determined by GPC method using polystyrene as standard and tetrahydrofuran as eluent at 30 °C (Table 1). The relatively large polydispersity index (PDI) of both polymers might originate from the aggregation in solution. The same issue was also reported for other polymers.[36,40]

But the new polymers have high molecular weights and they are sufficiently soluble for solution processing into thin film. Additionally, both polymers demonstrated excellent thermal stability, with 5% weight loss upon heating at 415 °C (Figure S1).

Optical and Electrochemical Properties. UV−vis−NIR absorption spectra of the polymers in solution and in film are shown in Figure 2. The relevant data are summarized in Table

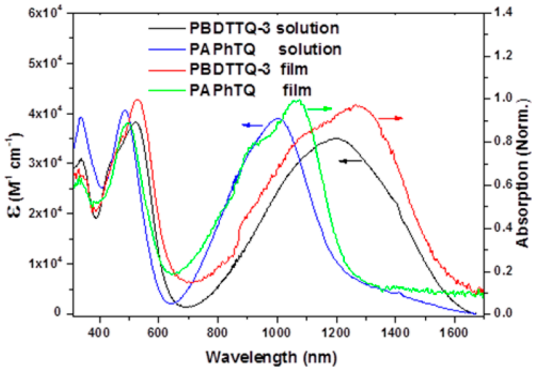

Figure 2. UV−visible−NIR absorption spectra of the polymers in chloroform solution and in films.

1. **PBDTTQ-3** exhibits an absorption maximum (λ_{max}) at 1206 nm in solution corresponding to a large red-shift of 278 nm as compared to that of **PBDTTQ-2**. On the other hand, the intensity of the lower energy band of **PBDTTQ-3** is significantly higher than that of **PBDTTQ-2** (not shown). This could be attributed to improved backbone coplanarity, leading to enhanced intramolecular charge transfer in solution of **PBDTTQ-3** after reducing the number of alkyl chains relative to **PBDTTQ-2**. Compared to **PBDTTQ-3**, the λ_{max} value of **PAPhTQ** reveals a blue shift of 201 nm indicating a weaker intramolecular charge transfer in **PAPhTQ** than for **PBDTTQ-3**, which thus possess the lowerbandgap. Thin films were prepared by drop-casting onto glass slides from chloroform solution. Both polymers displayed red-shifts of 64 and 67 nm at λ_{max} compared with those in solution suggesting aggregation in the solid state. The optical bandgaps are 0.76 and 0.99 eV, calculated according to the absorption onset of the solid films for **PBDTTQ-3** and **PAPhTQ**, respectively. These results demonstrate that modifying the alkyl chains and changing the aromatic condensed TQ core are effective tools in tuning the bandgaps of the polymers.

The electrochemical behaviors of both monomers and polymers were determined from cyclic voltammetry (CV) (Figure 3 and Supporting Information Figure S2). The data of

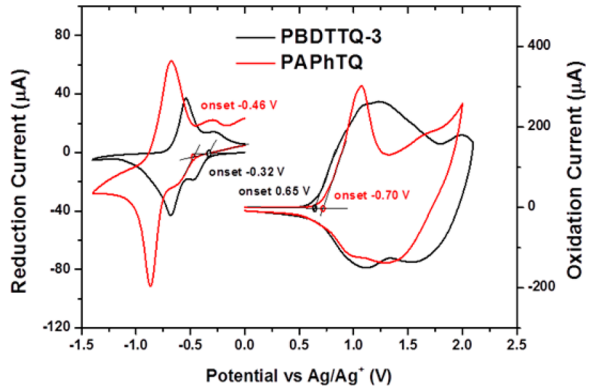

Figure 3. Reduction (left) and oxidation (right) of two polymers films deposited from chloroform solutions.

polymers were collected in Table 1. To avoid the electron withdrawing effects of bromine cyclic voltammetry of the acceptors, **BDTTQ-3** and **APhTQ** were carried out. The electron affinity (EA) of **BDTTQ-3** estimated from the reduction onset potential[41] is −3.92 eV, which is higher than that of **APhTQ** (−3.73 eV). This proved that **BDTTQ-3** is a stronger electron acceptor than **APhTQ**. The CV of the drop casted thin films of the polymers provided the EA values of −4.08 and −3.94 eV for **PBDTTQ-3** and **PAPhTQ**, respectively, whereas the ionization potential (IP) values of −5.05 eV for **PBDTTQ-3** and −5.10 eV for **PAPhTQ** were derived from the onset of the oxidation potential. These results proved that the benzodithiophene group made this TQ derivative become a stronger electron acceptor than acenaphthylene on the TQ segment, resulting in the lower EA of **PBDTTQ-3** compared to **PAPhTQ**. The EA of **PBDTTQ-3**

dx.doi.org/10.1021/cm502563t | *Chem. Mater.* 2014, 26, 5923−5929

was found around 0.14 eV lower than that of **PAPhTQ**, while the IP of the two polymers were nearly equivalent due to a dominant contribution of the tetrathiophene units to the IP for each polymer. Both polymers exhibited two reversible reductions and low EA, indicating their potential for electron charge carrier transport. The electrochemical band gaps of the polymers are larger than the optical band gaps, which is attributed to the exciton binding energy of conjugated polymers.[42]

To further understand the electronic structures and optical properties of the polymers, density functional theory (DFT) calculations were carried out. In agreement with the CV results similar HOMO levels were found for the two monomers **APhTQ** and **BDTTQ-3**, but there were striking differences in the LUMO values (Supporting Information Figure S3) with lower LUMO for **BDTTQ-3**. Also for the dimers of **BDTTQ-2**, **BDTTQ-3** and **APhTQ** the electronic density distributions of the LUMO and HOMO were derived from DFT analysis as shown in Supporting Information Figure S4. The dihedral angle for the 3,3′-dimethyl-2,2′-bithiophene in the dimer of **BDTTQ-2** is slightly larger, while it is computed to be only ∼7° for 2,2′-bithiophene in **BDTTQ-3**. The more effective extension of the π-conjugation in the latter case is due to the reduced number of alkyl chain interactions and therefore affords the smaller band gap as also confirmed by UV−vis−NIR. The HOMO and LUMO levels of three polymers, on the other hand, show very similar degrees of delocalization. Even when considering a large dihedral angle between the central two alkylated thiophenes in the dimer **BDTTQ-2** the electron densities are nearly equivalent. It should be mentioned that the twisting angle of these polymers will be smaller in the solid state than determined by DFT calculations.

OFET Properties. Bottom contact, bottom gate transistors were fabricated to investigate the charge carrier transport for both polymers. The ambipolar behavior of **PBDTTQ-3** is clearly evident from the transfer curves in both p- and n-type operation modes for negative and positive gate voltages, with average mobilities of 0.19 ± 0.03 $cm^2 V^{-1} s^{-1}$ for holes and 0.10 ± 0.07 $cm^2 V^{-1} s^{-1}$ for electrons (Table 1). In the negative drain mode for V_D < 0 V (Figure 4a) the crossover point is

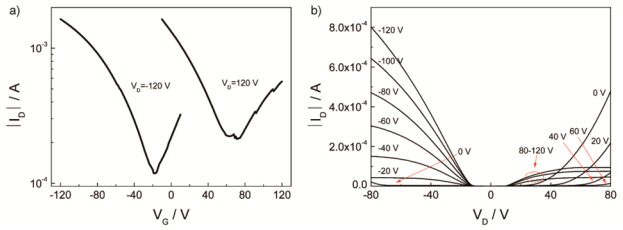

Figure 4. Transfer (a) and output (b) curves of **PBDTTQ-3**.

located at around V_G = −20 V, indicating a change from electron- to hole-dominated current. Below this gate voltage the transistor exhibits a typical hole transport behavior in the accumulation mode. In the positive regime at V_D > 0 V (Figure 4a) the electrons dominate the device operation up from approximately V_G = 70 V. The high crossover voltage can be attributed to two parallel existing effects: charge trapping at semiconductor/dielectric interface and contact resistance. The proposed mechanism for the trapping of electrons in the conductive channel is the formation of immobile $Si-O^-$ ions at the dielectric surface. Self-assembled monolayers (SAMs) lead to a reduced number of hydroxy groups and thus to an increase of the electron current.[5] The hexamethyldisilazane (HMDS) surface modification can reduce the trapping effect but not hinder it completely. Moreover, the contact resistance is evident on the output characteristic (Figure 4b) from the nonlinear behavior of the current at low V_D. In spite of this negative effect, the ambipolar device behavior was observed due to the low band gap and LUMO level, reaching highest values of 0.22 $cm^2 V^{-1} s^{-1}$ and 0.21 $cm^2 V^{-1} s^{-1}$ for holes and electrons, respectively. A well-balanced transport of holes and electrons for **PBDTTQ-3** is observed, whereas significant differences in threshold voltage are attributed to the deep traps existing in semiconducting layer.[43] Polymer **PAPhTQ** reveals also ambipolarity but with slightly lower average mobilities for holes of 0.10 ± 0.02 $cm^2 V^{-1} s^{-1}$ and with significant difference for electrons of 0.02 ± 0.01 $cm^2 V^{-1} s^{-1}$ (Supporting Information Figure S5). As previously studied, the air stable region of materials is below around −4.3 eV of EA.[44] Obviously, the EA of our polymers is not in this range and is the reason for the observation of only a hole transport after 1 h in air with highest mobilities of 0.11 and 0.09 $cm^2 V^{-1} s^{-1}$ for **PBDTTQ-3** and **PAPhTQ**, respectively (Supporting Information Figure S6).

Self-Organization. To gain an insight into the organization of both polymers in the bulk, 2DWAXS (Figure 5a,b) was

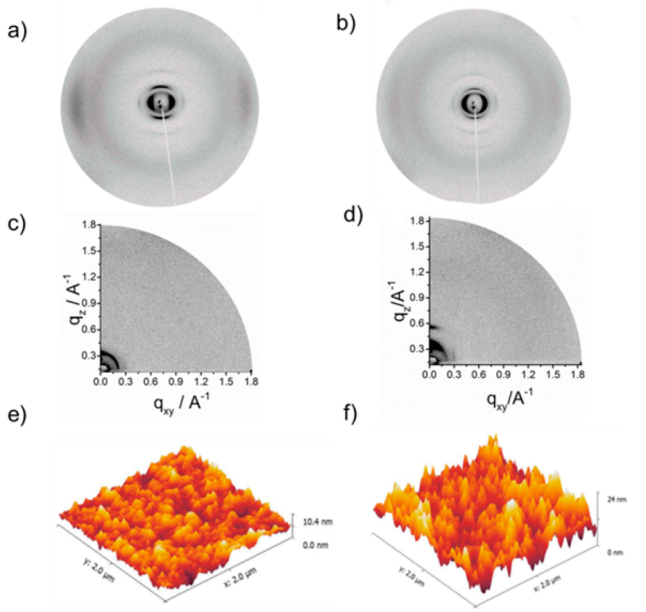

Figure 5. 2DWAXS patterns for extruded fibers of (a) **PBDTTQ-3** and (b) **PAPhTQ**. The fiber sample was mounted vertically toward the detector. GIWAXS patterns for (c) **PBDTTQ-3** and (d) **PAPhTQ** thin films. SFM topography images of **PBDTTQ-3** (e) and **PAPhTQ** (f) thin film in the transistor channel. The RMS roughness values are 1.3 nm for **PBDTTQ-3** film and 3.3 nm for **PAPhTQ** film, respectively.

carried out. The 2DWAXS measurements were performed on extruded fibers which were subsequently thermally annealed at 180 °C. The 2D patterns are quite identical for both compounds where reflections at small angles on the equatorial plane of the pattern are ascribed to polymer chains oriented along the alignment direction of the fiber. The chain-to-chain distance between lamellae of 2.73 nm for **PBDTTQ-3** and 2.5 nm for **PAPhTQ** are determined from the main peak positions.

dx.doi.org/10.1021/cm502563t | *Chem. Mater.* 2014, 26, 5923−5929

Meridional reflections corresponding to a *d*-spacing of 1.80 nm are equal for both systems and are attributed to the length of a single repeat unit. More crucially, wide-angle, equatorial scattering intensities are assigned to a relatively small π-stacking distance of 0.36 nm for both polymers which might be one factor responsible for the good charge carrier transport. However, this reflection is significantly weaker for **PAPhTQ** than for **PBDTTQ-3** (see Figure 4a,b), which indicates slightly less ordering, which might be one of the reasons for the lower mobility of **PAPhTQ**.

To understand the surface organization and morphology in thin film, GIWAXS and SFM were additionally performed (Figure 5c–f). For these measurements the same procedure for the film preparation was used as for the transistor devices. The GIWAXS pattern for **PBDTTQ-3** reveals only one isotropic reflection which correlates well with the chain-to-chain spacing of 2.73 nm of randomly arranged lamellas toward the surface. The thin film of **PAPhTQ** displays a slightly higher order and enhanced orientation of the polymer chains. The meridional scattering intensity at q_{xy} = 0 Å^{-1} and q_z = 0.27 Å^{-1} is attributed to the chain-to-chain spacing of 2.33 nm of edge-on arranged polymer backbones. The reflection at q_{xy} =0.31 Å^{-1} and q_z = 0 Å^{-1} corresponds to the length of a single repeat unit. In both cases, the HMDS modified silicon dioxide surface slightly decreases the chain-to-chain distance; however, the lack of a π-stacking reflection is evidence for poor packing of the polymers on the surface in comparison to the bulk. This indicates that strong $\pi-\pi$ stacking may not be always necessary for reaching high charge carrier mobilities. Some high performing semiconducting polymers also were reported with less ordered or disordered morphology.[45−48] In order to investigate the film structure in the nanometer scale we performed SFM on films obtained after drop-casting and annealing at 180 °C (Figure 5e,f). The root-mean-square (RMS) surface roughness of the **PAPhTQ** film was determined to be 3.3 nm, being significantly higher than that one of a **PBDTTQ-3** film (RMS = 1.3 nm). This difference indicates that **PBDTTQ-3** shows better order at the air interface. As reported in the literature, a high surface roughness indicates that large domains cause a nonuniform transport layer, and thereby it is limiting the conduction. Smoother polymer films, on the other hand, provide a higher uniformity due to smaller grain microstructures which lead finally to higher charge carrier mobilities.[49] This may be a reason why **PBDTTQ-3** has a higher mobility than **PAPhTQ**.

CONCLUSION

In summary, we have presented two new D−A copolymers based on an extended TQ core with a high molecular weight and good solubility in common solvents. Changing the electron donor of the fused aromatic system from acenaphthylene to benzodithiophene in the TQ moiety plays a significant role on the optoelectronic properties and the device performance. **PBDTTQ-3** exhibits balanced ambipolar charge carrier transport with transistor mobilities up to 0.22 cm^2 V^{-1} s^{-1} for holes and 0.21 cm^2 V^{-1} s^{-1} for electrons. To the best of our knowledge, these values are the highest among TQ-containing semiconductors. Interestingly, these mobilities were obtained for a quite disordered thin film as evident from GIWAXS measurements. A high performance of a disordered conjugated polymer might bear great potential for roll-to-roll printing, in which the microstructure and packing need to be less sensitive toward rapid processing conditions.

ASSOCIATED CONTENT

Supporting Information

Detail of materials characterization and the spectra of TGA, cyclic voltammograms, and NMR. This material is available free of charge via the Internet at http://pubs.acs.org.

AUTHOR INFORMATION

Corresponding Author

*(M.B.) E-mail: martin.baumgarten@mpip-mainz.mpg.de.

Notes

The authors declare no competing financial interest.

ACKNOWLEDGMENTS

This work is supported by SFB-TR49. C.A. and D.L. gratefully acknowledge the China Scholarship Council (CSC) for offering a Scholarship. T.M. and M.L. acknowledge the ERC Advanced Grant NANOGRAPH (AdG-2010-267160).

REFERENCES

(1) Kelley, T. W.; Baude, P. F.; Gerlach, C.; Ender, D. E.; Muyres, D.; Haase, M. A.; Vogel, D. E.; Theiss, S. D. *Chem. Mater.* **2004**, *16*, 4413.
(2) Forrest, S. R. *Nature* **2004**, *428*, 911.
(3) Tsao, H. N.; Cho, D. M.; Park, I.; Hansen, M. R.; Mavrinskiy, A.; Yoon, D. Y.; Graf, R.; Pisula, W.; Spiess, H. W.; Müllen, K. *J. Am. Chem. Soc.* **2011**, *133*, 2605.
(4) Capelli, R.; Toffanin, S.; Generali, G.; Usta, H.; Facchetti, A.; Muccini, M. *Nat. Mater.* **2010**, *9*, 496.
(5) Chua, L.-L.; Zaumseil, J.; Chang, J.-F.; Ou, E. C. W.; Ho, P. K. H.; Sirringhaus, H.; Friend, R. H. *Nature* **2005**, *434*, 194.
(6) Steckler, T. T.; Zhang, X.; Hwang, J.; Honeyager, R.; Ohira, S.; Zhang, X.-H.; Grant, A.; Ellinger, S.; Odom, S. A.; Sweat, D.; Tanner, D. B.; Rinzler, A. G.; Barlow, S.; Brédas, J.-L.; Kippelen, B.; Marder, S. R.; Reynolds, J. R. *J. Am. Chem. Soc.* **2009**, *131*, 2824.
(7) Fan, J.; Yuen, J. D.; Wang, M. F.; Seifter, J.; Seo, J. H.; Mohebbi, A. R.; Zakhidov, D.; Heeger, A.; Wudl, F. *Adv. Mater.* **2012**, *24*, 2186.
(8) Yuen, J. D.; Fan, J.; Seifter, J.; Lim, B.; Hufschmid, R.; Heeger, A. J.; Wudl, F. *J. Am. Chem. Soc.* **2011**, *133*, 20799.
(9) Chen, H.; Guo, Y.; Mao, Z.; Yu, G.; Huang, J.; Zhao, Y.; Liu, Y. *Chem. Mater.* **2013**, *25*, 3589.
(10) Chen, Z. Y.; Lee, M. J.; Ashraf, R. S.; Gu, Y.; Albert-Seifried, S.; Nielsen, M. M.; Schroeder, B.; Anthopoulos, T. D.; Heeney, M.; McCulloch, I.; Sirringhaus, H. *Adv. Mater.* **2012**, *24*, 647.
(11) Sonar, P.; Foong, T. R. B.; Singh, S. P.; Li, Y. N.; Dodabalapur, A. *Chem. Commun.* **2012**, *48*, 8383.
(12) Lee, J.; Han, A. R.; Yu, H.; Shin, T. J.; Yang, C.; Oh, J. H. *J. Am. Chem. Soc.* **2013**, *135*, 9540.
(13) Lei, T.; Dou, J. H.; Ma, Z. J.; Yao, C. H.; Liu, C. J.; Wang, J. Y.; Pei, J. *J. Am. Chem. Soc.* **2012**, *134*, 20025.
(14) Lei, T.; Dou, J.-H.; Cao, X.-Y.; Wang, J.-Y.; Pei, J. *Adv. Mater.* **2013**, *25*, 6589.
(15) Kitamura, C.; Tanaka, S.; Yamashita, Y. *Chem. Mater.* **1996**, *8*, 570.
(16) Inganäs, O.; Zhang, F. L.; Andersson, M. R. *Acc. Chem. Res.* **2009**, *42*, 1731.
(17) Chen, M. X.; Perzon, E.; Robisson, N.; Jönsson, S. K. M.; Andersson, M. R.; Fahlman, M.; Berggren, M. *Synth. Met.* **2004**, *146*, 233.
(18) Admassie, S.; Inganäs, O.; Mammo, W.; Perzon, E.; Andersson, M. R. *Synth. Met.* **2006**, *156*, 614.
(19) Cheng, K.-F.; Chueh, C.-C.; Lin, C.-H.; Chen, W.-C. *J. Polym. Sci., Part A: Polym. Chem.* **2008**, *46*, 6305.
(20) Sun, M.; Jiang, X.; Wang, L.; He, C.; Du, B.; Yang, R.; Cao, Y. *J. Polym. Sci., Part A: Polym. Chem.* **2008**, *46*, 3007.
(21) Yi, H.; Johnson, R. G.; Iraqi, A.; Mohamad, D.; Royce, R.; Lidzey, D. G. *Macromol. Rapid Commun.* **2008**, *29*, 1804.

(22) Yu, C.-Y.; Chen, C.-P.; Chan, S.-H.; Hwang, G.-W.; Ting, C. *Chem. Mater.* **2009**, *21*, 3262.
(23) Zoombelt, A. P.; Fonrodona, M.; Wienk, M. M.; Sieval, A. B.; Hummelen, J. C.; Janssen, R. A. J. *Org. Lett.* **2009**, *11*, 903.
(24) Cai, T.; Zhou, Y.; Wang, E.; Hellström, S.; Zhang, F.; Xu, S.; Inganäs, O.; Andersson, M. R. *Sol. Energy Mater. Sol. Cells* **2010**, *94*, 1275.
(25) Inganäs, O.; Zhang, F.; Tvingstedt, K.; Andersson, L. M.; Hellström, S.; Andersson, M. R. *Adv. Mater.* **2010**, *22*, E100.
(26) Zhang, X.; Steckler, T. T.; Dasari, R. R.; Ohira, S.; Potscavage, W. J.; Tiwari, S. P.; Coppee, S.; Ellinger, S.; Barlow, S.; Bredas, J.-L.; Kippelen, B.; Reynolds, J. R.; Marder, S. R. *J. Mater. Chem.* **2010**, *20*, 123.
(27) Dallos, T.; Beckmann, D.; Brunklaus, G.; Baumgarten, M. *J. Am. Chem. Soc.* **2011**, *133*, 13898.
(28) Dexter Tam, T. L.; Salim, T.; Li, H.; Zhou, F.; Mhaisalkar, S. G.; Su, H.; Lam, Y. M.; Grimsdale, A. C. *J. Mater. Chem.* **2012**, *22*, 18528.
(29) Lee, Y.; Jo, W. H. *J. Phys. Chem. C* **2012**, *116*, 8379.
(30) Keshtov, M. L.; Marochkin, D. V.; Kochurov, V. S.; Khokhlov, A. R.; Koukaras, E. N.; Sharma, G. D. *Polym. Chem.* **2013**, *4*, 4033.
(31) Steckler, T. T.; Fenwick, O.; Lockwood, T.; Andersson, M. R.; Cacialli, F. *Macromol. Rapid Commun.* **2013**, *34*, 990.
(32) Steckler, T. T.; Henriksson, P.; Mollinger, S.; Lundin, A.; Salleo, A.; Andersson, M. R. *J. Am. Chem. Soc.* **2014**, *136*, 1190.
(33) An, C.; Puniredd, S. R.; Guo, X.; Stelzig, T.; Zhao, Y.; Pisula, W.; Baumgarten, M. *Macromolecules* **2014**, *47*, 979.
(34) Beaujuge, P. M.; Tsao, H. N.; Hansen, M. R.; Amb, C. M.; Risko, C.; Subbiah, J.; Choudhury, K. R.; Mavrinskiy, A.; Pisula, W.; Bredas, J. L.; So, F.; Müllen, K.; Reynods, J. R. *J. Am. Chem. Soc.* **2012**, *134*, 8944.
(35) Chen, H.; Guo, Y.; Yu, G.; Zhao, Y.; Zhang, J.; Gao, D.; Liu, H.; Liu, Y. *Adv. Mater.* **2012**, *24*, 4618.
(36) Osaka, I.; Shimawaki, M.; Mori, H.; Doi, I.; Miyazaki, E.; Koganezawa, T.; Takimiya, K. *J. Am. Chem. Soc.* **2012**, *134*, 3498.
(37) Pisula, W.; Kastler, M.; Wasserfallen, D.; Pakula, T.; Müllen, K. *J. Am. Chem. Soc.* **2004**, *126*, 8074.
(38) Arroyave, F. A.; Richard, C. A.; Reynolds, J. R. *Org. Lett.* **2012**, *14*, 6138.
(39) Goto, H.; Akagi, K. *Angew. Chem., Int. Ed.* **2005**, *44*, 4322.
(40) Guo, X.; Puniredd, S. R.; Baumgarten, M.; Pisula, W.; Müllen, K. *Adv. Mater.* **2013**, *25*, 5467.
(41) Bredas, J.-L. *Mater. Horiz.* **2014**, *1*, 17.
(42) Sariciftci, N. S. *Primary Photoexcitations in Conjugated Polymers:Molecular Excitons vs Semiconductor Band Model*; World Scientific: Singapore, 1997.
(43) Braga, D.; Horowitz, G. *Adv. Mater.* **2009**, *21*, 1473.
(44) Jones, B. A.; Facchetti, A.; Wasielewski, M. R.; Marks, T. J. *J. Am. Chem. Soc.* **2007**, *129*, 15259.
(45) Osaka, I.; Zhang, R.; Sauvé, G. v.; Smilgies, D.-M.; Kowalewski, T.; McCullough, R. D. *J. Am. Chem. Soc.* **2009**, *131*, 2521.
(46) Osaka, I.; Zhang, R.; Liu, J.; Smilgies, D.-M.; Kowalewski, T.; McCullough, R. D. *Chem. Mater.* **2010**, *22*, 4191.
(47) Yuen, J. D.; Kumar, R.; Zakhidov, D.; Seifter, J.; Lim, B.; Heeger, A.; Wudl, F. *Adv. Mater.* **2011**, *23*, 3875.
(48) Ko, S.; Verploegen, E.; Hong, S.; Mondal, R.; Hoke, E. T.; Toney, M. F.; McGehee, M. D.; Bao, Z. *J. Am. Chem. Soc.* **2011**, *133*, 16722.
(49) Liu, J.; Zhang, R.; Osaka, I.; Mishra, S.; Javier, A. E.; Smilgies, D.-M.; Kowalewski, T.; McCullough, R. D. *Adv. Funct. Mater.* **2009**, *19*, 3427.